A Solvated Transition State for the Nucleophilic Attack on Cationic η^3-Allylpalladium Complexes

Helena Hagelin,[b] Björn Åkermark,[b] and Per-Ola Norrby*[a]

Abstract: Solvated transition states have been located for the title reaction by employing continuum solvation models together with high-level quantum chemical calculations. In most cases, there exists no corresponding gas phase barrier as a result of the very high in vacuo exothermicity for reaction of two ionic species with opposite charges. For the single case when a neutral model nucleophile was employed, the in vacuo transition state could be located and compared to the corresponding solvated transition state. There was a substantial difference between the transition states calculated in vacuo and in solution, both in terms of structure and energy. The implications of the results for the prediction of selectivities in palladium-assisted allylic alkylation are discussed.

Keywords: allylic alkylation · palladium · solvent effects · transition metals · transition states

Introduction

Palladium-assisted allylation is one of the most thoroughly investigated metal-mediated reactions.[1] The reaction pathway via an intermediate η^3-allyl complex is well proven (Scheme 1), and much is known about how different ligands and reaction conditions influence the observed selectivities.[2]

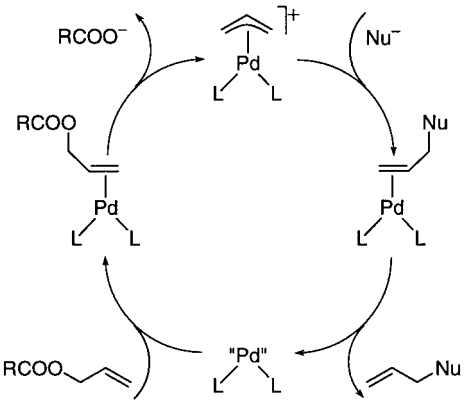

Scheme 1. The catalytic cycle of palladium-assisted allylic alkylation.

[a] Prof. Dr. P.-O. Norrby
Department of Medicinal Chemistry
Royal Danish School of Pharmacy
Universitetsparken 2, DK-2100 Copenhagen (Denmark)
Fax: (+45) 35-37-22-09
E-mail: peon@medchem.dfh.dk

[b] Prof. Dr. B. Åkermark, H. Hagelin, M.Sc.
Department of Chemistry, Organic Chemistry
Royal Institute of Technology
S-10044 Stockholm (Sweden)

Recently, there has been much interest in the development of new ligands for enantioselective allylation.[3–5] In several cases, specific ligand–substrate combinations have yielded enantioselectivities of at least 98%.[5, 6]

Rational development of new ligands, both for general and specific substrates, requires a deep understanding of the factors which influence the selectivity of the reaction. In the catalytic cycle of the allylation, the selectivity-determining step may vary depending on the substrates and the conditions.[4] In most cases, the rate-determining step will be either the addition of Pd^0 to the allylic substrate (commonly an allylic carboxylate) or a nucleophilic attack on the intermediate η^3-allylpalladium complex. The latter step is actually the reverse of the former, and differs only in the nature of the nucleophile/leaving group (Scheme 1, top). In a simplified view, both reactions can be seen as an S_N2 exchange between palladium and a nucleophile, in which palladium is already coordinated to the π-bond.

Previous theoretical studies of the title reaction have largely concentrated on the ground state properties of the η^3-allylpalladium complex. For example, the reactivity has been estimated from semiempirical calculations of the frontier orbitals in the allyl moiety,[7] whereas the effect of ligands and allyl substituents on the reactivity has been studied at higher levels of theory.[8] Several studies have dealt with the competition between the attack at the terminal and the central allyl carbon atom.[9] We know of only one study in which a transition state has actually been located for the attack of an external nucleophile (ammonia) on an η^3-allylpalladium complex.[10] The related transition state for the migration of a palladium-coordinated hydride to the allyl group (with retention of configuration at the carbon atom)

0947-6539/99/0503-0902 $ 17.50+.50/0

has also been studied.[11] When the reaction is used to form new carbon–carbon bonds, the leaving group is usually an anionic carboxylate and the nucleophile is a stabilized carbanion. In none of these cases can a transition state be located by standard high-level quantum mechanical calculations: the reaction between an anionic nucleophile and a cationic allylpalladium complex does not seem to have a barrier in the gas phase (vide infra). The barrier observed in real reactions can largely be attributed to desolvation work of the reacting ions.

We have recently shown that selectivities in palladium allylation reactions can be predicted well by a linear free energy relationship (LFER) based on the calculated structures of the ground-state η^3-allylpalladium complex together with a few postulates about the transition-state geometry.[12] The model was able to produce good predictions, but it was limited to a narrow range of reaction conditions. In order to make more general predictions possible, we set out to base our modeling on a more accurate description of the transition state. As a first step towards such a model, we report herein the determination of transition-state geometries for the reaction of a cationic η^3-allylpalladium complex with a range of nucleophiles relevant to the two transition states leading to and from the η^3-allylpalladium complex in the Pd-catalyzed allylation cycle (Scheme 2).

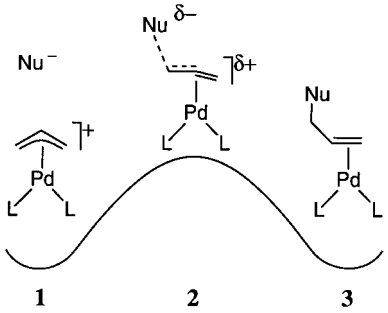

Scheme 2. Transition state for the reaction of a η^3-allyl complex with a nucleophile or, in reverse, for the formation of η^3-allyl from an olefin complex (Nu = leaving group).

Computational Models

The title reaction has been shown to work well with a wide range of ligands, including amines. It has recently been shown that excellent selectivities can be obtained in the title reaction by the use of suitably substituted bidentate nitrogen ligands.[5, 6a–c] We have chosen to use two ammonia molecules as a simple model of a bidentate nitrogen ligand in our calculations.

There is a plethora of nucleophiles and leaving groups that can be utilized in the palladium-catalyzed allylation. The leaving group usually has an electronegative atom connected to the allyl moiety, and it leaves as a negative ion (e.g. chloride or carboxylate). The most common nucleophiles are probably stabilized carbanions, but neutral heteroatom nucleophiles, such as amines, are also frequently employed.[2] To cover as broad a range as possible, it was decided to investigate the reaction of three different nucleophiles with the η^3-allylpalladium moiety: one electronegative anion, one stabilized carbon anion, and one neutral amine. In order to limit the conformational degrees of freedom as much as possible, and also to minimize the size of the quantum chemical calculations, the final choice fell on the fluoride anion, the cyanide anion, and ammonia.

All calculations were performed with the hybrid B3LYP functional[13] in Gaussian 94.[14] The B3LYP method has repeatedly been shown to yield results that are at least equal to MP2 calculations.[15] For geometry optimizations, we have employed the LANL2DZ basis set for all atoms. For Pd, this basis set consists of the small core ECP of Hay and Wadt,[16] with a [341/321/31] contracted valence set. The use of a pseudorelativistic effective core potential for second-row transition metals generally improves the results compared to all-electron nonrelativistic calculations, and at a much lower computational cost.[17] B3LYP/LANL2DZ seems to be a reasonable minimum level for the calculation of geometries and crude energies of organometallic complexes. For single point energies and solvation calculations, a larger polarized basis set was utilized. For palladium the same ECP was employed, together with a [3311/3111/211/1] contraction for the valence set (we used one f-polarization function taken from the literature[18]). For all other atoms, the 6-31G* basis was used. Fluorine was given an extra diffuse function (i.e., 6-31 + G*). All energies reported in this work were obtained with the larger basis set.

Two main methods are available for the treatment of solvation in molecular modeling: inclusion of explicit solvent molecules in the calculation, or the use of a continuum solvation model.[19] In the current work, we employed the latter method. The former method is used extensively in molecular dynamics calculations, but must be modified for quantum chemical implementation. Microsolvation by one or a few solvation molecules has been employed in the study of anionic nucleophiles;[20] however, for the inclusion of a representative ensemble of solvation molecules, it is necessary to couple the quantum chemical representation of the solute to classical force field representations of the solvent molecules (QM/MM methods).[21]

Several continuum solvation models are available for quantum chemical calculations; they range from simple electrostatic interaction with the surrounding solvent to methods which also include the free energy terms from cavitation, van der Waals interactions, etc.[19] Continuum models, in general, describe the average interaction between a solute and an equilibrated solvent. Of the methods available to us, we chose to employ the PCM/DIR model from Tomasi et al.,[22] and the SM2 model from Cramer, Truhlar et al.[23] The models are quite different in how they treat the interaction between the solute and the solvent; however, they both modify the Hamiltonian and allow the solute wavefunction to respond to solvation. Both models also include explicit treatment of the dispersion interactions and cavitation work, based on a calculated solvent-accessible surface area (SASA). The PCM model is based on a polarizable cavity surrounding the solute, and has been implemented for use with the Gaussian 94 program[14] (it should not be confused with the various PCM models available in standard Gaussian 94). Of the many solvents that have been parameterized in the PCM/DIR model, we chose to use dichloromethane and water. The SM2 model for water solvation, based on the generalized Born equation, was developed for use with semiempirical AM1 wavefunctions.[24] It was not possible to include the full complex in the SM2 calculations, as no parameters were available for the solvation of palladium. The palladium with the two auxiliary ligands was therefore removed, whereupon relative SM2 solvation energies were calculated for the resulting allyl cation–nucleophile complexes. The differences between the AM1/SM2 and the gas-phase AM1 single point energies were then added to the corresponding gas phase energies, obtained with the larger basis set, in order to yield approximate SM2 energies. We want to point out that as a result of the heavy truncation of the model system, the SM2 energies were not expected to be accurate. However, on account of the ease of use, the negligible computational requirements, and the high availability of the method, we still wanted to test it as a source of quick, qualitative solvation estimates.

Neither of the utilized solvation methods allowed the direct calculation of the energy derivatives for the full complex. Without access to analytical gradients, the direct determination of the transition states or intermediates could not be accomplished in practice. Neither could the transition state structures be located in the gas phase. In order to calculate a solvated reaction pathway, we therefore had to fix the reaction coordinate, relax the remaining degrees of freedom in the gas phase, and subsequently calculate the solvated energy for the final geometry. The procedure is based on the assumption that relaxation of the geometry in a solvent would yield a similar energy decrease for all species, without major conformational changes. The latter is probably true, as the conformational freedom in the model system is very limited. For widely differing points on the reaction pathway, the relaxation may give very different results, especially considering that the reaction goes from an ionic to a neutral complex (Scheme 2). Therefore, the calculated overall heat of reaction should be treated with caution.

  0947-6539/99/0503-0903 $ 17.50+.50/0

Continuum models based on cavities surrounding the solute are sensitive to the size of the cavity, and thus to both solute atomic radii and the solvent radius used in the determination of the SASA. For bimolecular reactions, the models would be expected to show discontinuities at the point where the two separate cavities merge. For cavity-based methods in general, this region could be troublesome, not only for transition states, but also for weakly bonded systems (e.g. hydrogen bonds or van der Waals contacts) where the cavity surfaces lie very close to each other. When the interatomic distance is slightly higher than the sum of the cavity radii, there were will be a narrow slit between the two cavities. For slit sizes of one molecule or less, treatment of the volume in the slit as a continuous dielectric will clearly be nonphysical. When the interatomic distance is lowered to the sum of the cavity radii, the SASA will discontinuously start to vary strongly with interatomic distance, as the intersecting parts of the cavities will be removed from the calculation. We have therefore carefully verified that no discontinuities exist in the calculated solvation energies close to the calculated transition states. For the PCM model, discontinuities were found, but only well beyond the transition states. In all cases, the final transition states were contained within one cavity. Points beyond the discontinuity were not used in the determination of the transition-state geometry and energy (vide infra).

The obvious choice for the reaction coordinate was the distance between the terminal allyl carbon and the nucleophile. However, with geometry optimizations performed in the gas phase, this single coordinate was found to be insufficient. The anionic nucleophiles are very strong bases in the gas phase,[25] and this problem was exaggerated by the use of a relatively small basis set. At certain fixed distances, the base was strong enough to abstract an allyl proton. For fluoride, even the addition of a diffuse function was insufficient to inhibit the proton abstraction. Assuming that the problem would be alleviated by the inclusion of solvation effects, it was decided to add a second reaction coordinate, with the expectation that a barrier would be found at the extremes of the new coordinate on the *solvated* potential energy surface (PES). There were three reasonable choices for a second reaction coordinate: the Pd-C-Nu angle, the C-C-Nu angle, or the Pd-C-C-Nu dihedral angle. The last choice was found to be the best to limit interactions with the allyl protons and to avoid problems with multiple minima. The sign of the dihedral angle is defined as positive when the approach vector is tilted in the direction of the *anti* substituent (Scheme 3).

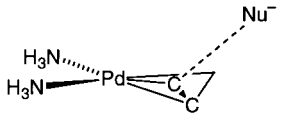

Scheme 3. Nucleophilic attack on the model complex. The dihedral angle Pd-C-C-Nu (the angle between the Pd-C-C and the C-C-Nu planes, where the C atoms considered are the central and the reacting allyl carbons) is defined as positive when the nucleophile is close to the *anti* substituent.

Scans of the potential energy surface were performed in two dimensions, with geometry optimizations performed at the B3LYP/LANL2DZ level. The step sizes were 0.1 Å for the C–Nu distance and 10° for the dihedral angle Pd-C-C-Nu. Gas-phase and solvation energies were determined by single-point calculations (vide supra). The approximate location of the transition state was then located graphically. A few badly converged outliers were removed, whereupon a second-degree polynomial was fitted to all data points within 0.3 Å of the approximate TS. The final position of the TS was then determined by analytic solution of the polynomial. Geometrical features of the TS (e.g. bond lengths) were determined by linear interpolation of the four closest structures on the PES.

For the neutral nucleophile ammonia, it has been shown previously that the reaction indeed exhibits a gas phase barrier.[10] The transition state was also identified in the current system on the unsolvated B3LYP/LANL2DZ PES. The stationary point was located by the QST2 routine in Gaussian 94.

Results

The gas-phase transition state for the nucleophilic attack of ammonia on the model complex is discussed first, as here the results from interpolations on the PES can be compared to a true TS. A plot of the polynomial which results from a fit to the data points closest to the TS is shown in Figure 1. The largest deviation of any data point from the surface is 0.7 kJ mol^{-1}. Solution of the polynomial yields the coordinates (1.93 Å, 164°) for the transition state. The true transition state was located by the use of the coordinates (1.8 Å, 170°) and (2.0 Å, 160°) as starting structures for the synchronous transit search. The final structure, shown in Figure 2, has the

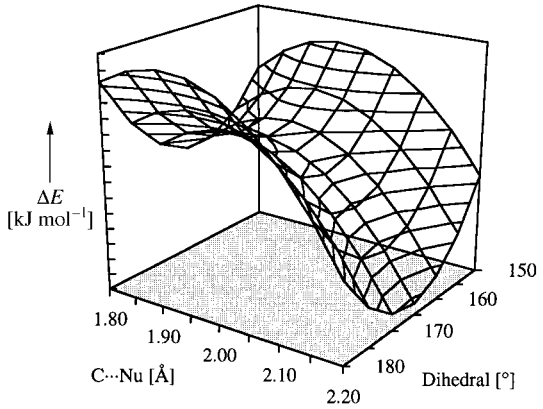

Figure 1. Fitted PES for the addition of NH_3 to the (η^3-allyl)Pd complex in the gas phase.

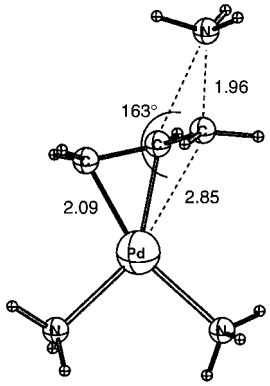

Figure 2. The gas-phase transition state for the addition of NH_3 to the model η^3-allyl complex.

coordinates (1.96 Å, 163°), with a C–C···N angle of 109.7°. We note that in the study of combined PN ligands performed by Blöchl and Togni,[10] the transition structure for the attack of NH_3 *trans* to a nitrogen ligand displayed a C···N distance of 1.932 Å and a C-C···N angle of 109.5°, which is very similar to the current structures, despite the differences in ligands and methodology.

Three sets of solvation energies were added to the gas phase energies. When NH_3 is used as the nucleophile, the entire system is cationic; however, the charge is less localized in intermediate structures than in any endpoint structure. Delocalization of the charge generally gives rise to less efficient solvation by continuum models and leads to an increase in the relative energy for the middle section of the PES. A typical PES, resulting from a polynomial fit to energies in dichloromethane, is shown in Figure 3.

We now turn to systems with anionic nucleophiles: here we found potential energy surfaces that decreased monotonously

0947-6539/99/0503-0904 $ 17.50+.50/0 *Chem. Eur. J.* **1999**, *5*, No. 3

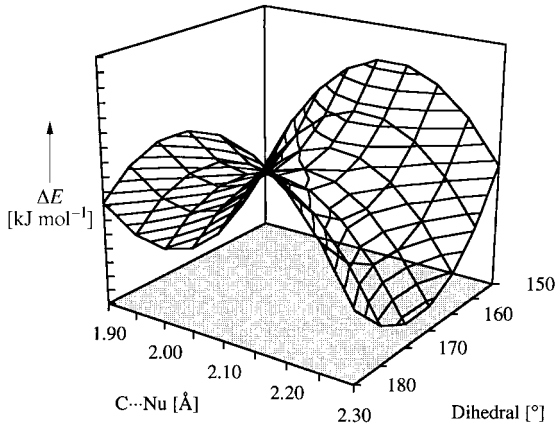

Figure 3. PES for the addition of ammonia in dichloromethane, calculated with the PCM solvation model.

in energy as the nucleophile approached the cationic (η^3-allyl)Pd complex. However, the separated ions are preferentially stabilized by the solvation methods. It was possible to locate transition states for all solvated systems, which yielded surfaces similar to the one depicted in Figure 3.

Table 1. Reaction coordinates for all stationary points.[a]

Structure model	Nu C_r–Nu [Å]	Solvation Pd-C_c-C_r-Nu [°]		
2[b]	NH_3	none	1.959	163.1
2	NH_3	none	1.934	164.0
2	NH_3	CH_2Cl_2	2.104	165.6
2	NH_3	H_2O (PCM)	2.115	166.5
2	NH_3	H_2O (SM2)	2.100	165.2
3[b]	NH_3	none	1.634	159.4
2	F^-	CH_2Cl_2	2.060	166.6
2	F^-	H_2O (PCM)	1.984	161.1
2	F^-	H_2O (SM2)	2.184	168.0
3[b]	F^-	none	1.495	169.9
2	^-CN	CH_2Cl_2	2.393	167.9
2	^-CN	H_2O(PCM)	2.317	166.2
2	^-CN	H_2O(SM2)	2.259	166.6
3[b]	^-CN	none	1.482	170.6

[a] Except where noted, these were determined from a polynomial fit to calculated energies. [b] True gas phase structure, not fitted.

The final coordinates for all stationary points on the two-dimensional reaction surfaces, obtained from an analytical solution of the fitted polynomials, can be found in Table 1. Selected structural elements of all transition states, as well as the (η^3-allyl)Pd complex and the three Pd(olefin) complexes, are shown in Table 2 and the energies for each stationary point relative to the reactants (**1**) are given in Table 3.

Discussion

Reaction energetics: It has long been known that there is a profound difference between the reaction profiles in the gas phase and in solution. In particular, localized ions will be preferentially stabilized by solvation. The effect is found in any solvent, but is stronger in polar or hydrogen-bonding environments. For most solutes, there is also a correlation between the solvation energy and the surface area, which favors extended conformations and dissociated complexes. On the other hand, increasing the solute volume is disfavored on account of the cavitation work. The latter effect will selectively disfavor transition states involved in bond breaking. The volume increase upon bond elongation will generally require more energy than that gained by the simultaneous increase in area.

Table 3. Reaction barriers and energies of products **3** and transition states **2** relative to the reactants **1**.

Nu	Solvation model	ΔE (**3** – **1**) [kJ mol^{-1}]	ΔE^* (**2** – **1**) [kJ mol^{-1}]
NH_3	none	2	9
NH_3	CH_2Cl_2	– 3	33
NH_3	H_2O(PCM)	4	47
NH_3	H_2O(SM2)	– 10	38
F^-	none	– 469	–
F^-	CH_2Cl_2	47	72
F^-	H_2O(PCM)	87	117
F^-	H_2O(SM2)	209	280
^-CN	none	– 548	–
^-CN	CH_2Cl_2	– 119	29
^-CN	H_2O(PCM)	– 69	71
^-CN	H_2O(SM2)	13	137

Table 2. Selected geometrical descriptors of all stationary points.[a]

Structure	Nu	Solvation model	Pd–C_c [Å]	Pd–C_t [Å]	Pd–C_r [Å]	C_c–C_t [Å]	C_c–C_r [Å]	Pd-C_r-Nu [°]	C_c-C_r-Nu [°]	δ C_r[b] [Å]
1[c]	none	none	2.225	2.207	2.205	1.425	1.425	–	–	0.151
2[c]	NH_3	none	2.183	2.092	2.854	1.452	1.439	153.9	109.7	0.910
2	NH_3	none	2.178	2.092	2.872	1.452	1.443	153.4	109.8	0.926
2	NH_3	CH_2Cl_2	2.197	2.105	2.717	1.447	1.425	158.2	109.0	0.760
2	NH_3	H_2O(PCM)	2.197	2.107	2.703	1.447	1.425	159.0	108.8	0.743
2	NH_3	H_2O(SM2)	2.198	2.104	2.723	1.447	1.426	157.9	109.0	0.767
3[c]	NH_3	none	2.128	2.089	3.050	1.458	1.489	145.4	109.8	1.081
2	F^-	CH_2Cl_2	2.178	2.112	2.797	1.441	1.433	154.8	107.7	1.012
2	F^-	H_2O(PCM)	2.176	2.105	2.850	1.443	1.440	151.4	108.2	1.067
2	F^-	H_2O(SM2)	2.188	2.120	2.707	1.440	1.425	157.8	107.0	0.927
3[c]	F^-	none	2.128	2.108	3.039	1.443	1.495	150.2	111.1	1.163
2	^-CN	CH_2Cl_2	2.184	2.119	2.704	1.440	1.430	160.9	110.7	0.918
2	^-CN	H_2O(PCM)	2.178	2.113	2.771	1.442	1.436	158.2	111.0	0.988
2	^-CN	H_2O(SM2)	2.172	2.110	2.813	1.442	1.442	157.2	111.1	1.024
3[c]	^-CN	none	2.113	2.110	3.106	1.444	1.537	150.0	113.1	1.205

[a] Except where noted, all descriptors were determined by linear interpolation between the four closest calculated geometries. Allyl carbons are designated by lower indices c for central, t for nonreacting terminal, and r for reacting. [b] Distance of reacting carbon (C_r) to the N-Pd-N plane. [c] True gas phase structure, not interpolated.

In the case of the attack of ammonia on the cationic η^3-allylpalladium complexes, palladium will distribute the charge over all ligands; however, the charges in both the reactant and the product are still more localized than in the intermediate complexes on the reaction pathway (in particular the TS). The gas-phase and solution energetics are shown in Table 3, and the reaction profiles are depicted in Figure 4. It can be seen

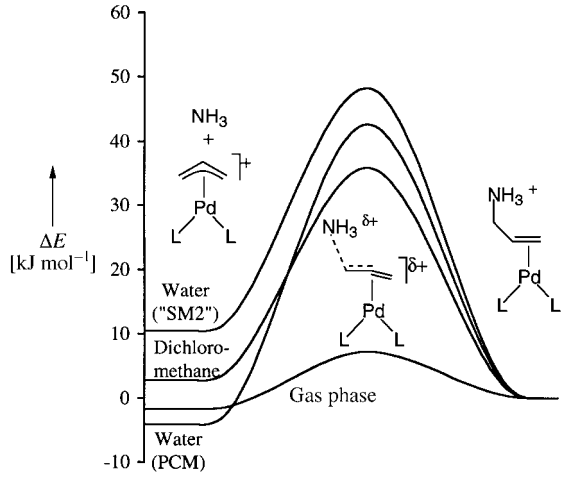

Figure 4. Reaction profiles for the attack of ammonia upon the η^3-allylpalladium complex. Only the energies of stationary points are represented, not the position of the transition states.

that the reaction is essentially thermoneutral, with a only a negligible barrier in the gas phase. The change in the reaction energy upon solvation (maximally 12 kJ mol^{-1}) is small compared to the accuracy of the methods employed, especially when considering that relaxation of the gas phase geometries in the solvent has been neglected. It is somewhat surprising that the dissociated complex is not favored by solvation; however, the increase in the surface area is counteracted by a delocalization of the positive charge, so that the difference in the total solvation energy is close to zero.

The reaction barrier is significantly increased by solvation, as expected from the preceding arguments. However, the total reaction barrier is still low, both for association and dissociation. As the reaction is bimolecular, the dissociated complex is expected to be favored by approximately 30 kJ mol^{-1} at room temperature on account of the entropy contribution. Extrapolation of these results to amine nucleophiles indicates that the allylation of amines that contain active hydrogens will yield allylic amines as a result of the rapid deprotonation of the initial product, which will shift the equilibrium towards product. On the other hand, tertiary amines can be leaving groups in the generation of cationic η^3-allylpalladium complexes from allyl ammonium salts,[2, 26] in accordance with the current results.

There is a surprisingly close correspondence between the various solvation models for all cases when ammonia is used as the nucleophile. A comparison of the two PCM models indicates that all the species are more strongly solvated in the water model, with the total solvation energies almost twice as high as those obtained from the dichloromethane model. Despite this, the relative solvation energies are very similar in the two models. The reaction barrier is increased and the energy of the dissociated complex is lower in water relative to dichloromethane, as expected for a more polar solvent, but the differences are small.

The PCM models depend on a numerical integration over the surface area of the molecule. As a result of this, small errors are introduced when geometries with unequal surfaces are compared. The effect is most easily seen in the quality of the fit of the polynomial PES to the calculated data points. The standard errors were 0.6 – 0.7 kJ mol^{-1} for the fit to PCM energies. The SM2 model does not suffer from the same problem, thus the calculated surface was smoother and the standard error for the fit slightly lower (0.5 kJ mol^{-1}). The total solvation energies were substantially larger for the SM2 model than for any of the PCM models; however, this can be attributed solely to the removal of the metal. The free allyl cation will have a substantially stronger localized charge than the η^3-allylpalladium complex, and therefore a stronger solvation contribution. Despite the drastic approximations, the transition state coordinates from the SM2 model were very close to those obtained from the PCM models.

We now consider anionic nucleophiles: profiles for addition of fluoride are shown Figure 5 and for addition of cyanide in Figure 6. As expected for combinations of ion pairs in the gas

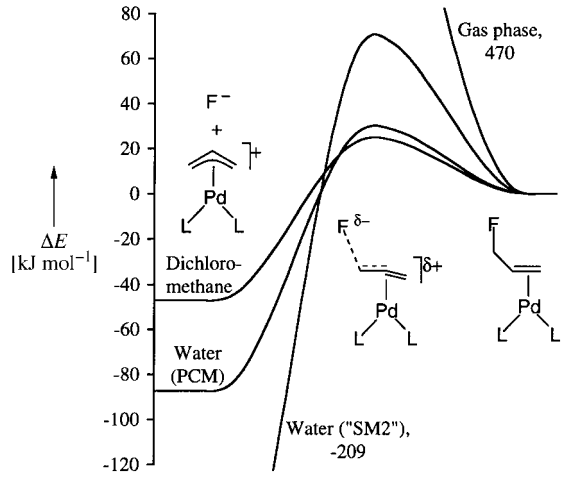

Figure 5. Profiles for the attack of fluoride.

phase, both reactions are very exothermic. It can be noted that the results from the SM2 model now diverge from the PCM models, and strongly favors the dissociated ions in both cases. Again, the divergence from the PCM model is probably due to the removal of the metal, not to the solvation methods as such.

The addition of the fluoride anion to the η^3-allylpalladium complex is endothermic in all solvated systems, as a consequence of the very efficient solvation of the free ions. When entropy effects are included, it is clear that dissociation is very favorable and has a low barrier. Other electronegative elements may be less well solvated than the fluoride ion, but they also form weaker bonds to carbon. It should therefore be possible to extrapolate the current results to other electronegative leaving groups, in good agreement with the observation that substrates, such as allylic chlorides, esters, and even alcohols, react with Pd^0 to form (η^3-allyl)Pd complexes in good yield.[1]

0947-6539/99/0503-0906 $ 17.50+.50/0 *Chem. Eur. J.* **1999**, *5*, No. 3

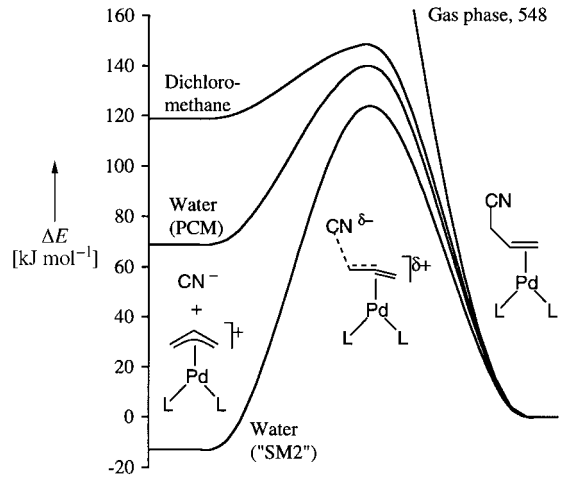

Figure 6. Profiles for the attack of cyanide.

The addition of cyanide to the η^3-allylpalladium complex is exothermic according to both PCM models. The Pd(olefin) product should therefore be favored, even if the expected entropic contribution of $\approx 30\ kJ\ mol^{-1}$ at room temperature is included. The calculated potential energy barrier to addition is only $\approx 30\ kJ\ mol^{-1}$ in dichloromethane. The addition of stabilized carbon nucleophiles in solvents of low polarity is therefore expected to be facile, which is in good agreement with experimental observations.

Transition state geometries: We have previously shown that the selectivities in Pd-assisted alkylation of stabilized carbanions in dichloromethane can be rationalized by geometrical features of the intermediate η^3-allylpalladium complex,[12] with the assumption that the observed distortions would correlate with the geometrical features of the transition state. The most significant geometry elements were: 1) steric interactions with a large probe on the $Pd-C_r$ vector, 3.0 Å from C_r (the reacting carbon), 2) elongation of the $Pd-C_r$ bond, and 3) rotation of the allyl towards a product-like conformation. Each of these will now be analyzed in the light of the current results, in particular those from the addition of cyanide in dichloromethane.

Steric interaction with the incoming nucleophile: In our previous modeling based on molecular mechanics, a large probe (an argon atom) was employed, which experienced full nonbonded interactions with all parts of the allyl group. With those approximations, it was found that a distance of 3.0 Å to the probe yielded good results. In the current study, all transition states show a substantially shorter C_r-Nu distance (the longest, but also the most relevant, is ≈ 2.4 Å for the addition of cyanide in dichloromethane). However, the nucleophile in the current study is smaller, and some of the nonbonded interactions should have been replaced by bonded interactions in the transition state. The C_c-C_r-Nu angles observed here ($\approx 110^\circ$, Table 2) are similar to those found in the molecular mechanics study; however, the Pd-C_r-Nu angle is lower than 180° ($\approx 150-160^\circ$, Table 2). This is caused by a tilt of the C_r-Nu vector towards the allyl *anti* substituent. However, as can be seen in Figure 2, the *anti* substituent has simultaneously bent towards the palladium, with the end result that the relative interactions of the nucleophile with the *syn* and *anti* substituents are in close agreement with previous findings. All in all, the steric interactions measured in our molecular mechanics study would be expected to correlate well with the true transition state interactions.

Elongation of the $Pd-C_r$ bond: From Table 2, it is clear that most bonds change very little on going from the reactant (η^3-allyl)palladium complex to the transition state. The sole exception is the cleavage of the $Pd-C_r$ bond, which generally is already very product-like in the transition state. An elongation of the bond in the ground state would therefore be expected to facilitate the formation of the transition state, as previously proposed.[3, 5] Interestingly, even the C_c-C_r bond, which should change from conjugated to single, is almost unchanged in the TS. It can also be noted that the coordinated double bond in the product (C_c-C_t) is slightly longer than the same bond in the (η^3-allyl)Pd complex, as a result of very strong back-bonding from palladium.

Rotation of the allyl relative to the coordination plane: in the Pd(olefin) product, the double bond lies almost exactly in the coordination plane of palladium, defined as the N-Pd-N plane (this can also be observed in solution and in crystal structures[27]). As a result, the reacting carbon (C_r) is displaced out of the coordination plane towards the former *anti* substituent by ≈ 1.2 Å (Table 2). In the reactant, the (η^3-allyl)Pd complex, the terminal carbons lie very close to the coordination plane ($\delta C_r \approx 0.15$ Å). With respect to this parameter, the transition state is reminiscent of the product, with $\delta C_r > 0.9$ Å for an attack by cyanide, in agreement with our previous studies. Interestingly, this parameter seems less important for the addition of neutral amine nucleophiles ($\delta C_r \approx 0.75$ Å).

Solvation models: The current application of the SM2 model is very crude, as the relative solvation contributions are determined from the AM1 wave function for fixed geometries of the free allyl without the stabilizing effect of the metal. Therefore, the correspondence between the transition state coordinates from the SM2 and the PCM water models is gratifying. The agreement was very close when ammonia was used as the nucleophile, and reasonably close in the case of cyanide. In our hands, the PCM water model and SM2 have yielded results of similar quality when applied to organic molecules. However, in this case, the PCM model could be applied to the entire system, so that the PCM results must be considered to be more reliable. Despite this, the SM2 model could be used to obtain qualitative results for simplified versions of organometallic complexes if computational resources are limited. The time required to determine SM2 solvation energies is completely insignificant compared to the high-level calculations, whereas the PCM calculations require approximately twice the CPU time of a gas phase calculation at the same level of theory.

Neither of the solvation methods used have been verified for use with transition metals, and only superficially for use with ionic systems. We have therefore been careful to employ

only relative solvation energies between similar systems. However, the positions of the transition states depend only on relative energies at adjacent points on the PES. Since in all cases the PES show a strong, continuous curvature close to the TS, the coordinates of the TS on the two-dimensional PES should be accurate to within a few percent.

Conclusions

We have used ammonia, fluoride, and cyanide as examples of neutral and anionic nucleophiles with different electronegativities to calculate the transition states for their addition to the cationic bis(amine)-η^3-allylpalladium(II) complex. In all cases, these transition states are clearly product-like. The major geometrical changes on going from η^3-allylpalladium complex to the transition state are: i) an elongation of the breaking Pd–C bond, ii) a rotation of the allyl to bring the olefin product into the N-Pd-N coordination plane, and iii) the bend of the *anti* substituent away from the approaching nucleophile. The results correlate well with a previous molecular mechanics study of selectivities in the palladium-assisted allylation.[12] As would be expected, inclusion of solvent interactions is crucial. In the gas phase, no transition state could be located for the highly exothermic additions of fluoride and cyanide anions. For ammonia, a gas-phase transition state could be located, but the reaction barrier was very low and a substantial change in the transition-state geometry was observed upon solvation. By the use of two solvation models, SM2 and PCM/DIR, reasonable transition states could be located with all three nucleophiles. Since our usage of SM2 is very crude, the similarity of the results from the two water models is very gratifying. Continuum solvation models are continuously being improved, and a few methods are available that will allow calculation of analytical gradients for geometry optimizations within the solvation model. So far, we have found none that will work with transition metal complexes, but we expect these to appear in the near future. The impact on computational organometallic chemistry should be substantial.

With respect to the palladium-catalyzed allylic alkylation, the availability of a transition-state geometry should aid the understanding and prediction of experimental selectivities. With the current results as a guide, we plan to continue our long-range project of creating a predictive selectivity model for experimentally interesting systems. Selectivity predictions in this system could now be implemented as QSAR-type models, based on either the reactant or the product geometries,[12] Jensen-type interpolations[28] calibrated against the current results, which use recently developed molecular mechanics force fields for both reactant[29] and product,[30] or as true molecular mechanics transition-state models based on the geometries determined here.

Acknowledgments

Financial support from the Danish Medical Research Council, the Danish Technical Research Council, the Carl Trygger Foundation, and the Swedish Research Council for Engineering Sciences is gratefully acknowledged. H.H. also wishes to thank the Ernst Johnson Foundation for a scholarship.

[1] a) B. M. Trost, T. R. Verhoeven in *Comprehensive Organometallic Chemistry, Vol. 8* (Eds.: G. Wilkinson, F. G. A. Stone, E. W. Abel), Pergamon, Oxford, **1982**, 799; b) R. F. Heck, *Palladium Reagents in Organic Synthesis*, Academic Press, New York, **1985**.
[2] P. J. Harrington in *Comprehensive Organometallic Chemistry II, Vol. 12* (Eds.: E. W. Abel, F. G. A. Stone, G. Wilkinson, L. S. Hegedus), Pergamon, Oxford, **1995**, 797.
[3] a) C. G. Frost, J. Howarth, J. M. J. Williams, *Tetrahedron: Asymmetry* **1992**, *3,* 1089; b) O. Reiser, *Angew. Chem.* **1993**, *105*, 576; *Angew. Chem. Int. Ed. Engl.* **1993**, *32,* 547.
[4] B. M. Trost, D. L. van Vranken, *Chem. Rev.* **1996**, *96*, 395.
[5] a) A. Pfaltz, *Acta Chem. Scand.* **1996**, *50,* 189; b) A. K. Ghosh, P. Mathivanan, J. Cappiello, *Tetrahedron: Asymmetry* **1998**, *9,* 1.
[6] a) D. Tanner, A. Harden, F. Johansson, P. Wyatt, P. G. Andersson, *Acta Chem. Scand.* **1996**, *50,* 361; b) K.Nordström, M. Macedo, C. Moberg, *J. Org. Chem.* **1997**, *62,* 1604; c) G. Chelucci, *Tetrahedron: Asymmetry* **1997**, *8,* 2667; d) P. von Matt, A. Pfaltz, *Angew. Chem.* **1993**, *105*, 614; *Angew. Chem. Int. Ed. Engl.* **1993**, *32*, 566; e) J. Sprinz, G. Helmchen, *Tetrahedron Lett.* **1993**, *34,* 1769; f) J. M. Brown, D. I. Hulmes, P. J. Guiry, *Tetrahedron* **1994**, *50,* 4493; g) J. Sprinz, M. Kiefer, G. Helmchen, M. Reggelin, G. Huttner, O. Walter, L. Zsolnai, *Tetrahedron Lett.* **1994**, *35,* 1523; h) G. J. Dawson, J. M. J. Williams, S. J. Coote, *Tetrahedron: Asymmetry* **1995**, *6,* 2535; i) G. J. Dawson, J. M. J. Williams, S. J. Coote, *Tetrahedron Lett.* **1995**, *36,* 461; j) A. Togni, U. Burckhardt, V. Gramlich, P. S. Pregosin, R. Salzmann, *J. Am. Chem. Soc.* **1996**, *118*, 1031; k) U. Burckhardt, V. Gramlich, P. Hofmann, R. Nesper, P. S. Pregosin, R. Salzmann, A. Togni, *Organometallics* **1996**, *15,* 3496; l) W. Zhang, T. Hirao, I. Ikeda, *Tetrahedron Lett.* **1996**, *37,* 4545.
[7] a) S.Sakaki, M. Nishikawa, A. Ohyoshi, *J. Am. Chem. Soc.* **1980**, *102*, 4062; b) M. Curtis, D. O. Eisenstein, *Organometallics* **1984**, *3*, 887; c) T. R. Ward, *Organometallics* **1996**, *15*, 2836.
[8] a) K. J. Szabó, *Organometallics* **1996**, *15*, 1128; b) K. J. Szabó, *J. Am. Chem. Soc.* **1996**, *118*, 7818; c) K. J. Szabó, E. Hupe, A. L. E. Larsson, *Organometallics* **1997**, *16*, 3779.
[9] a) C. Carfagna, R. Galarini, K. Linn, J. A. López, C. Mealli, A. Musco *Organometallics*, **1993**, *12*, 3019; b) A.Aranyos, K. J. Szabó, A. M. Castano, J.-E. Bäckvall, *Organometallics* **1997**, *16*, 1058.
[10] P. E.Blöchl, A. Togni, *Organometallics* **1996**, *15*, 4125.
[11] S. Sakaki, H. Satoh, H. Shono, Y. Ujino, *Organometallics* **1996**, *15*, 1713.
[12] J. D.Oslob, B. Åkermark, P. Helquist, P.-O. Norrby, *Organometallics* **1997**, *16,* 3015.
[13] a) A. D. Becke, *J. Chem. Phys.* **1993**, *98,* 5648; b) C. Lee, W. Yang, R. G. Parr, *Phys. Rev. B* **1988**, *37,* 785.
[14] Gaussian 94, Revision B.3, M. J. Frisch, G. W. Trucks, H. B. Schlegel, P. M. W. Gill, B. G. Johnson, M. A. Robb, J. R. Cheeseman, T. Keith, G. A. Petersson, J. A. Montgomery, K. Raghavachari, M. A. Al-Laham, V. G. Zakrzewski, J. V. Ortiz, J. B. Foresman, C. Y. Peng, P. Y. Ayala, W. Chen, M. W. Wong, J. L. Andres, E. S. Replogle, R. Gomperts, R. L. Martin, D. J. Fox, J. S. Binkley, D. J. Defrees, J. Baker, J. P. Stewart, M. Head-Gordon, C. Gonzalez, and J. A. Pople, Gaussian Inc., Pittsburgh PA, **1995**.
[15] B3LYP frequently gives an accuracy equal to or higher than MP2, both for ground and transition state properties: a) J. B.Foresman, Æ. Frisch, *Exploring Chemistry with Electronic Structure Methods,* 2nd ed., Gaussian Inc., Pittsburgh, **1996**; b) M. J. Frisch, presentation at the 213th ACS National Meeting, San Fransisco, **1997**; c) D. A. Singleton, S. R. Merrigan, J. Liu, K. N. Houk, *J. Am. Chem. Soc.* **1997**, *119,* 3385.
[16] P. J. Hay, W. R. Wadt, *J. Chem. Phys.* **1985**, *82*, 299.
[17] a) G. Frenking, I. Antes, M. Böhme, S. Dapprich, A. W. Ehlers, V. Jonas, A. Neuhaus, M. Otto, R. Stegmann, A. Veldkamp, S. F. Vyboishchikov in *Rev. Comp. Chem., Vol. 8* (Eds.: K. B. Lipkowitz, D. B. Boyd), VCH, New York, **1996**, 63; b) T. R. Cundari, M. T. Benson, M. L. Lutz, S. O. Sommerer in *Rev. Comp. Chem., Vol. 8* (Eds.: K. B. Lipkowitz, D. B. Boyd), VCH, New York, **1996**, 145.
[18] A. W. Ehlers, M. Böhme, S. Dapprich, A. Gobbi, A. Höllwarth, V. Jonas, K. F. Köhler, R. Stegmann, A. Veldkamp, G. Frenking, *Chem. Phys. Lett.* **1993**, *208*, 111.
[19] a) J. Tomasi, M. Persico, *Chem. Rev.* **1994**, *94,* 2027; b) C. J. Cramer, D. G. Truhlar in *Rev. Comp. Chem., Vol. 6* (Eds.: K. B. Lipkowitz, D. B. Boyd), VCH, New York, **1995**, 1.

  0947-6539/99/0503-0908 $ 17.50+.50/0 *Chem. Eur. J.* **1999**, *5*, No. 3

[20] a) P. E. M. Siegbahn, *Organometallics* **1997**, *16*, 6021; b) P. E. M. Siegbahn, *J. Phys. Chem. A* **1996**, *100*, 14672; c) F. M. Bickelhaupt, E. J. Baerends, N. M. M. Nibbering, *Chem. Eur. J.* **1996**, *2,* 196.
[21] J. Gao in *Rev. Comp. Chem., Vol. 7* (Eds.: K. B. Lipkowitz, D. B. Boyd), VCH, New York, **1995**, 119.
[22] PCM/DIR version 2.0, implementation for Gaussian 94 Rev. B.3, courtesy of Dr. Maurizio Cossi: M. Cossi, V. Barone, R. Cammi, J. Tomasi, *Chem. Phys. Lett.* **1996**, *255,* 327.
[23] C. J. Cramer, D. G. Truhlar, *Science* **1992**, *256*, 213.
[24] AM1/SM2 implemented in Spartan SGI version 4. 0.3 GL, Wavefunction Inc., 18401 von Karman, suite 370, Irvine, CA 92715.
[25] Fluoride has been shown to have a very high proton affinity in the gas phase: S. Gronert, G. N. Merrill, S. R. Kass, *J. Org. Chem*. **1995**, *60*, 488.
[26] R. Malet, M. Morena-Mañas, R. Peixats, *Organometallics* **1994**, *13*, 397.
[27] The geometry of the primary reaction product, the Pd(olefin) complex, has been determined by NMR: H. Steinhagen, M. Reggelin, G. Helmchen, *Angew. Chem.* **1997**, *109*, 2199; *Angew. Chem. Int. Ed. Engl.* **1997**, *36,* 2108. A few palladium(0)-olefin crystal structures can be found in the Cambridge Crystallographic Database. Original Publications as follows: CARJOU: H. Werner, G. T. Crisp, P. W. Jolly, H.-J. Kraus, C. Kruger, *Organometallics* **1983**, *2*, 1369; FICBIC: M. Hodgson, D. Parker, R. J. Taylor, G. Ferguson, *J. Chem. Soc. Chem. Comm*. **1987**, 1309; GENJAK: M. A. Bennett, C. Chiraratvatana, G. B. Robertson, U. Tooptakong, *Organometallics* **1988**, *7*, 1403; SOLTAO: R. Benn, P. Betz, R. Goddard, P. W. Jolly, N. Kokel, C. Kruger, I. Topalovic, *Z.Naturforsch., Teil B* **1991**, *46*, 1395.
[28] F. Jensen, *J. Comp. Chem.*, **1994**, *15*, 1199.
[29] P.-O. Norrby, H. Hagelin, B. Åkermark, unpublished results.
[30] P.-O. Norrby, H. Hagelin, B. Åkermark, unpublished results.

Received: May 18, 1998
Revised version: October 15, 1998 [F1165]